MECHANISMS OF PRECIPITATES FORMATION IN AN Al- Cu- Li- Zr ALLOY USING DSC TECHNIQUE AND ELECTRICAL RESISTANCE MEASUREMENTS

S. Ahmadi[1], H. Arabi[2], S. Nouri[3] and A. Shokuhfar[4]
sh.ahmadi@modares.ac.ir
Received: August 2008 Accepted: April 2009

[1] Department of Material Science, Faculty of Engineering, Tarbiat Modares University, Tehran, Iran.
[2] Center of Excellence of Advanced Materials and Processing (CEAMP), School of Metallurgy and Materials Engineering, Iran university of Science & Technology (IUST), Tehran, Iran.
[3] School of Metallurgy and Materials Engineering, Iran university of Science & Technology (IUST), Tehran, Iran.
[4] Department of Material Science, Faculty of Mechanical Engineering, K. N. Toosi University of Technology, Tehran, Iran.

Abstract: *Guinier-Preston (GP) zone formation and precipitation behavior of T1 (Al_2CuLi) phase during the ageing of an Al-Cu-Li-Zr alloy was studied by differential scanning calorimetry (DSC) technique and electrical resistance measurement of the samples. Results show that endothermic effects in the thermograms of the alloy between 180°C and 240°C can be related to the enthalpy of GP zones dissolution. Formation of GP zones in the structure increased hardness, tensile strength and electrical resistance of the Al-Cu-Li-Zr alloy. Furthermore, precipitation of T1 phase occurred in temperature range of 250ºC to 300ºC whereas its dissolution occurred within the temperature of 450-530ºC. Activation energies for precipitation and dissolution of T1 phase which were determined for the first time in this research, were 122.1(kJ/mol) and 130.3(kJ/mol) respectively. Results of electrical resistance measurements showed that an increase in the aging time resulted in the reduction of electrical resistance of the aged samples.*

Keywords*: aluminum- lithium alloys, DSC; activation energy, natural aging, Al-Cu-Li-Zr alloy, T1 phase, dissolution energies*

1. INTRODUCTION

In response to the demands of industries for the new materials with higher specific modulus and strength, aluminum- lithium alloys were developed. Aluminum –Lithium alloys such as 2090, 2091 and 8090 provide higher specific modulus than those of the previous grades of Aluminum alloys (e.g. 7075, 2024) and therefore replacements of some parts of aircrafts with these new alloys have been started at the same time [1-5].

Ageing process is the most important method to improve the mechanical properties of aluminum- lithium alloys. For example, in AA2090 alloy temperature ranges such as 70-120ºC and 150 -210ºC were used for natural and artificial ageing respectively in order to improve the mechanical properties [6, 7].

The precipitation sequence in AA 2090 alloy represented as: supersaturated solid solution → co-clusters → GP zones → θ'' → θ' → θ → T_1 [8, 9].

High volume fraction of metastable phases such as $\theta, \theta', \theta''$, T_1, T_2 and T_B are usually formed within the structure of Al-Li 2090 alloy after being subjected to artificial aging processes. However the major phase which has the significant effects on the properties of Al-Li 2090 alloy is said to be $T_1(Al_2CuLi)$ [10]. T_1 phase has hexagonal lattice and platelet morphology which can be formed during the ageing treatments at 135-260ºC.

The orientation relationship between T_1 phase and matrix has been presented by the following equations [11]:

$$(11\bar{2}0)_{T_1} \parallel (2\bar{1}\bar{1})_{Al}, \quad (0001)_{T_1} \parallel (111)_{Al}, \quad (10\bar{1}0)_{T_1} \parallel (\bar{1}\,\bar{1}0)_{Al}$$

Differential scanning calorimetry (DSC) has been effectively used for studying transformation

kinetics in aluminum alloys. By fitting a kinetic model to DSC or DIC (Differential Isothermal calorimetry) curves, the kinetic parameters, e.g. the activation energy (Ea) and rate constant (k) can be determined. For linear heating experiments, activation energies of reactions can be derived from a set of DSC experiments which performed at different heating rats (β). Kissinger peak method is widely used for determination of activation energies in the reactions when the temperatures of peaks can not be determined accurately due to overlapping heat effects [12, 13].

In this research, stability of GP zones and T_1 phase under the different aging conditions as well as the effects of GP zones on physical and mechanical properties of an Al-Cu-Li-Zr alloy sheet have been investigated by measuring its hardness, electrical resistant and tensile properties. Furthermore, for the first time activation energies for precipitation and dissolution of T_1 phase have been determined by performing the DSC experiments at different heating rates.

2. METHOD & MATERIALS

The hot rolled sheet of Al-2.35Cu-2.1Li- 0.1Zr (wt %) alloy with 0.1 wt% Fe and 0.1 wt% Si and a thickness of 2 mm was utilized for this investigation. The original sheet was cast (in a completely sealed furnace and argon atmosphere), homogenized, and hot rolled in several paths. Then it was solution annealed at 525°C for one hour and subsequent cold rolled (14 % reduction in thickness). Three sets of specimens were prepared from this sheet to the treated under various aging conditions. The first set of the specimens was aged either at 25°C (natural aging) or at 100°C after cold rolling. The aging treatments routs were as follows:

Solution Annealed + Natural Aged (40days) (1)

S.A. + 100°C/100hrs (2)

The specimens treated by the second rout, were aged either at 25°C (natural aging) or at 100°C prior to aging them at 150°C for 48 hrs. The overall aging treatments were as follow:

S.A. + N.A. (40days) + 150°C/48hrs (3)
S.A. + 100°C/100hrs + 150°C/48hrs (4)

The third set of the specimens were aged either at 150°C or at 190°C for different times after solution annealing according to the following routs.

S.A. + 150°C / 6-100 hrs (5)

S.A. + 190°C / 1-48 hrs (6)

Discs having dimension of 5mm diameter and 1mm thickness were prepared from the sheet mentioned for DSC examination. Scanning of the samples over the temperature rang of 25-1000°C at three different heating rates of 5, 10 and 15 °C/min were performed in a NEC-409pc calorimeter. Argon was used as both a purge and protective gas during DSC test. Base lines in differential scanning calorimetry tests were determined by not using any sample at all or using "empty pan" method.

Hardness tests were carried out on the aged specimens obtained from surfaces with #1000 grades SiC-paper. Electrical resistance was measured by a micro-ohmmeter device having 1 μΩ accuracy.

3. RESULTS AND DISCUSSION

3.1. Stability of GP zones

Fig. 1. illustrates the differential scanning calorimetry curves of solution annealed (at 520°C), aged at 100°C and room temperature (40 days) specimens. Some heat effects observed at temperatures lower than 250°C in the thermograms of aged samples. For example in the calorimetric diagram of 100°C/100 hrs specimen, the primary and final points of the endothermic pick occurred at: 180°C/-10.7mW and 240°C/-11.7mW respectively. On the other hand, endothermic effects between 180°C and 240°C which demonstrate the dissolution of precipitates or components can be seen in Fig. 1.

Therefore it can be suggested that all the endothermic effects in the DSC curves between

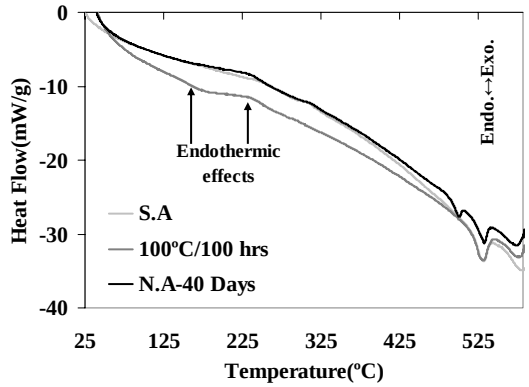

Fig. 1. Differential scanning calorimetry curves of the solution annealed, natural aged and artificial aged (100°C/100 hrs) specimens.

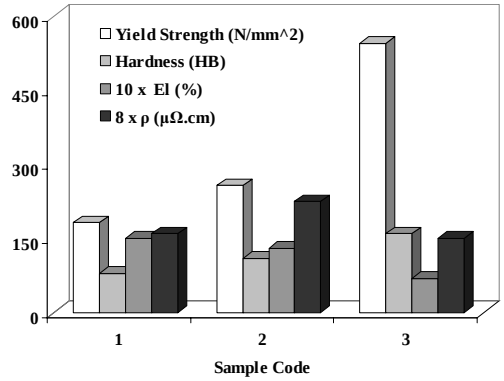

Fig. 2. The effect of heat treatment conditions on variation of hardness; electrical resistance; yield strength and elongation of Al-Cu-Li alloy. Sample code: 1- Solution annealed, 2- Natural aged (40 days), 3- Natural aged (40 days) + aged at 150°C for 48 hrs.

180°C and 240°C were due to dissolution of GP zones. In some other research performed for the low temperature aging process in Al alloys, endothermic picks in calorimetry examinations between 175°C and 240°C have been said to be related to dissolution of GP zones. Because of the short range diffusion of Cu atoms in the low temperature aging processes, formation and dissolution of Cu clusters in Al matrix has the lowest enthalpy among the other structural precipitates of Al alloys. Diffusion space of Cu atoms, X, can be calculated by means of eq. 7 [14-17]:

$$X^2 = D_0 \exp(-\frac{Q}{RT})\, t \qquad (7)$$

This leads to D_0=0.647 cm^2/s, Q=32.27 Kcal/mol

In fact, diffusion of Cu atoms in the aluminum matrix for low temperature aging process is almost in the atomic scale (a^{Al} = 3.61°A) and in this condition, clusters of Cu atoms formed in the structure. These clusters can be converted to GP zones by increasing the diffusion time.

Electrical resistance data are very useful tools for studying the initial stages of aging and provide indirect evidence on the interaction between solute atoms and precipitates. Effects of solute atoms on electron scattering are more important than those grain boundaries, dislocation, and precipitates according to G. Riontino [14] and N. Gao [16]. Solute atoms, clusters and GP zones disrupt electron flow through the lattice and decrease the conductivity. In Fig. 2 and Fig. 3 results of hardness, electrical resistant and tensile tests of the natural and artificial aged samples are shown. Stabilizing of GP zones in the structure of Al-Cu-Li alloy

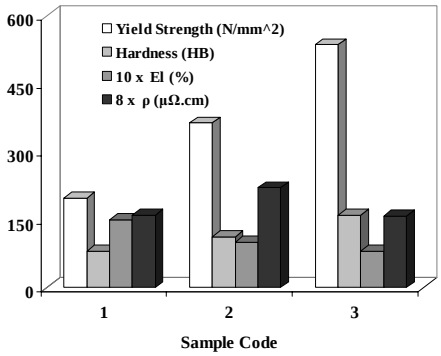

Fig. 3. The effect of heat treatment conditions on variation of hardness, electrical resistance, yield strength and elongation of Al-Cu-Li alloy. Sample code: 1- Solution annealed, 2- Artificial aged 100°C for 100hrs, 3- Artificial aged 100°C for 100hrs + aged at 150°C for 48 hrs.

increases the hardness, yield strength and electrical resistant.

3.2. Stability of T1 Phase

Fig. 4 demonstrates the variations in hardness of the alloy aged at 190ºC and 150ºC for different times (second set of the specimens). At ageing temperatures of 190ºC and 150ºC, the hardness gradually increased with the increase of ageing time and reached a maximum hardness of 170 HB and 168 HB after 12hrs and 48hrs aging time respectively. It is clear from the ageing curve that at higher temperature over ageing occurred in a shorter ageing time as expected. This behavior

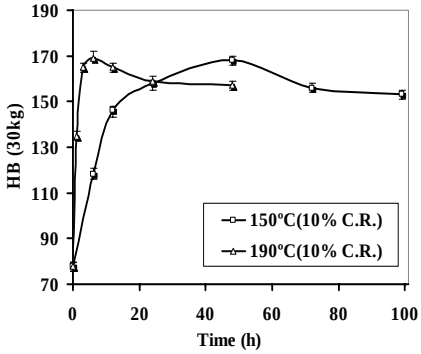

Fig. 4. Relation between hardness and aging time for two different temperatures used for aging treatment.

can be attributed to the mechanism of strain hardening in which the dislocation density increased by cold working and thus enhanced the diffusion rate, so that the precipitation rate of alloying elements increased in the microstructure by more dislocation interactions.

It appears that maximum of hardness occurred in the 190ºC/12 hrs aging condition and therefore this sample was selected for calorimetric studies.

In Fig. 5 results of the calorimetric test of 190ºC/12 hrs specimen in three different heating rates are shown within which the effects of hating rate on the DSC curves are presented. In all thermograms, main effects consist of; 1- exothermic effect at temperature range of 250-290°C, 2- endothermic effect at the range of 470-530°C and 3- endothermic effect at about 610°C to 660°C. The first peak shows an exothermic reaction that is due to the precipitation or the formation of phases whereas the second peak represents the endothermic effect due to the dissolution of compounds. The main endothermic peaks appeared around 650°C in DSC curves. In other research, this temperature was attributed to

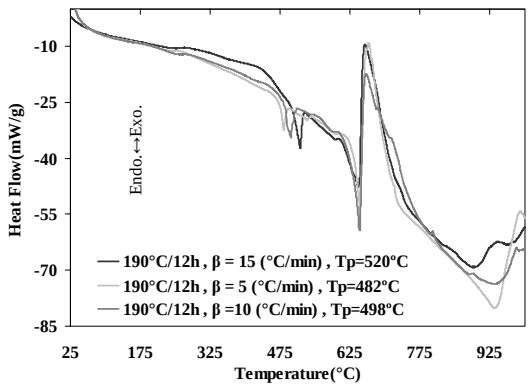

Fig. 5. DSC curves of the specimens aged at 190ºC in three different heating rates.

the melting point of AA2090 alloy [18, 19]. One also can observed in this figure that by increasing the heating rate, peak of precipitation (T_P^f) shifted from 255°C to 275°C while the peak of dissolution (T_P^d) shifted from 482°C to 520°C.

Effects of heating rate on precipitation of T_1 phase is presented in Fig. 6. Endothermic effects in the thermograms of Fig. 6 are an indication of dissolution of phases such as T_1, T_2, θ, θ' ' and T_B. T_1 (Al_2CuLi) phase was the predominant precipitate at temperatures between 135°C and 260°C in a similar research [11]. According to the research by Davydov and Fridlyander [20], temperature ranges for precipitation and dissolution of T_1 phase in the DSC curves are 275 - 310°C and 440 - 510°C respectively. Therefore, exothermic effects observed between 250ºC to 300ºC in this research can be attributed to precipitation of T_1 phase. The DSC diagrams at three heating rates show that TPf shift to higher temperatures by increasing heating rate (β). In Table 1, the amounts of T_P^f values for three heating rates are given.

Kissinger peak method was used for determination of activation energy in the precipitation and dissolution of T_1 phase. According to the equation 8, plotting ln (T_P^f/β) versus $1/T_P^f$ gives a straight line, the slope of which equals to E_a/R [15].

$$\ln \frac{T_P^2}{\beta} = \frac{E_a}{RT_P} + C \qquad (8)$$

Arrhenius plot for the maximum of the exothermic heat effects has been shown in Fig. 7. Slope of the precipitation line find from this figure was equal to 14.7 and therefore activation energy for the precipitation of T_1 phase was measured to be 122.1(kj/mol).

Endothermic effects in the temperature range of 450-530ºC in the DSC diagrams were attributed to dissolution of T_1 phase. In Fig. 6 variation of the heat effects for dissolution of T1 phase (T_P^d) for three different heating rates are shown and Table 2 gives the amounts of T_P^d for

Table 1. TPf for three heating rates measured for the sample aged at 190°C/12hrs.

Heating rate(ºC/min)	5	10	15
T_p(ºC)	255	270	275

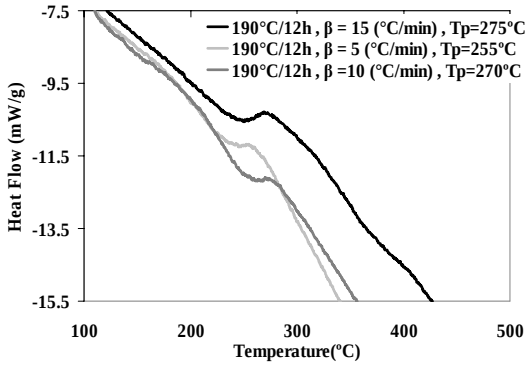

Fig. 6. Variation of T_p^f for three different heating rates.

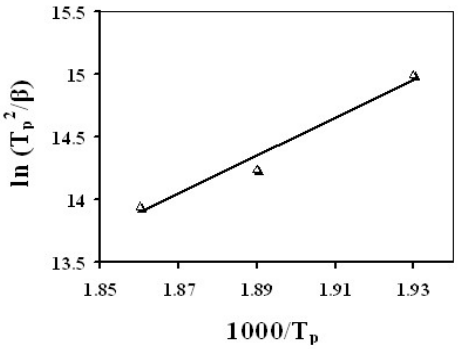

Fig. 7. Arrhenius plot of ln (T_P^2/ β) vs. 1000/TP) for precipitation of T1 phase.

Table 2. TPd in three heating rates for 190ºC/12h aged specimens.

Heating rate (ºC/min)	5	10	15
T_p(ºC)	482	498	520

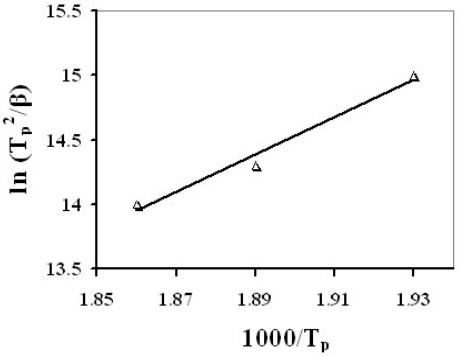

Fig. 8. Arrhenius plot of ln (T_P^2/ β) vs. (1000/TP) for dissolution of T1 phase.

the three heating rates. The slop of the line in Arrhenius plot (Fig. 8) for dissolution of T_1 phase was 15.7. Therefore, the activation energy for dissolution of T_1 phase was measured to be 130.3(kj/mol).

Activation energies observed for precipitation reactions within the temperature range 200-300ºC are closed to the activation energy for diffusion of precipitating elements (this is about 120-135 kJ/mol for Cu, Mg, Si). It is also reported that the activation energies for diffusion of Cu and Li atoms in Al are 135(kj/mol) and 130.1(kj/mol) respectively [13]. In fact, the activation energies obtained for precipitation and dissolution of T_1 phase in this study, i.e. 122.1(kj/mol) and 130.3(kj/mol), are very close to the activation energies reported for diffusion of alloying elements, i.e. Cu, Li and Mg in Al-base alloys. On the other hand, the results of this research show that the activation energies (calculated from DSC curves) for the precipitation reactions were equal to the activation energies for diffusion of these elements in Al-Cu-Li structure. This is an indication of the stability of some strengthening phases (e.g. T_1) with in the structure of the Al-Cu-Li alloy after the aging processes.

Fig. 9 demonstrates the electrical resistivities of aged specimens for various aging times. This Figure indicates that the electrical resistance of the samples decreased during the ageing treatments of alloy at both 190°C and 150°C. This seems to be due to the formation of the precipitates in the structure during the ageing process.

It should be noted here that the maximum of the electrical resistance belonged to the solution heat-treated samples whereas formation of the stable strengthening phases (such as T_1) by aging process caused the electrical resistance to

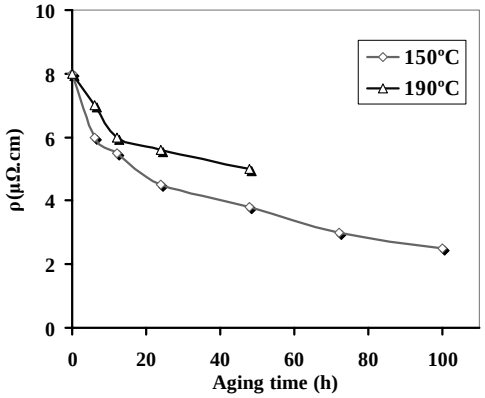

Fig. 9. Relation between electrical resistance and aging time.

decrease (i.e. electrical conductivity to increase).

4. CONCLUSIONS

1. Endothermic effects in the DSC curves of the Al-Cu-Li-Zr alloy with in the temperature range of 180-240°C thought to be due to the enthalpy of GP zones dissolution.
2. Exothermic effects within the temperature range 250-300ºC attributed to the precipitation; and endothermic effects between 450ºC and 530ºC to the dissolution of T_1 phase.
3. Activation energies for the precipitation and the dissolution of T_1 phase were 122.1(kJ/mol) and 130.3(kJ/mol) respectively. These values are almost equal to the activation energies for diffusion of Cu and Li elements in Al.
4. Low temperature aging process and formation of GP zones in the structure of Al- Cu-Li-Zr alloys increased the electrical resistance apparently by disrupting the electron flow through the lattice. Electrical resistance also decreased by increasing the aging time and temperature. This was probably due to a higher degree of precipitates formation.

REFERENCES

1. R. J. Rioja, Mater. Sci. & Eng A, 257, (1998), 100-107.
2. C. Meric, Mater. Research Bulletin, 35, (2000), 1479-1494.
3. J. A. Yurko, SAE International, (2003), 19.
4. E. S. Balmuth and R. Schmidt., The Metallurgy Society of AIME, Second International Aluminum- Lithium Conference in China, 1983, pp. 70-88.
5. I. N. Fridlyander, Mater. Sci. Forum, 331-337, (2000), 921
6. N. I. Kolobnev, L. B. Khokhlatova and I. N. Fridlyander: Mater. Forum, 28, (2004), 208-212.
7. K. Satya. A. A. Gokhale, A. K. Mukhopadhyay, D. Banerjee and D. B. Goel, Mater. Sci. Forum, Vols. 331-337, (2000), 1043-1048.
8. A. E. Smith and S. Homolya, Mater. Forum, 28, (2004), 139-144.
9. Y. Nagai, K. Hono, S. Yanagita, T. Honma and Hasegawa, Mater. Forum, 28, (2004), 287-292.
10. F. W. Gayle and B. Vandersande, Acta Materialia, 37, (No.4), (1989), 1033-1046.
11. P. S. Chen and B. N. Bhat: Alabama, NASA/TM-200-211548, (2002)
12. J. Yan, M. J. Starink. In: University of Southampton, SO17 IBJ, Materials Research Group, 2004, 31-33.
13. M. J. Starink: Int. Mater. Rev., 49, (2004), 191-226.
14. G. Riontino, S. Abis and Mengucci, Mater. Sci. Forum, 331-337, (2000), 1025-1030.
15. A. Gaber, K. Matsuda, Z. Yong, T. Kawabata, A. M. Ali and S. Ikeno, Mater. Forum, 28, (2004), 402-405.
16. N. Gao, M. J. Starink and L. Davin, Mater. Sci. Tech., 21, (2005), 1010-1018.
17. L. Davin, A. Cerezo, N. Gao and M. J. Statink, Surface and Interface Analysis, 36, (2004), 589-593.
18. S. Ahmadi, A. Shokuhfar, A. Rezaei, Defect and Diffusion Forum, 258-260, (2006), 15-19.
19. A. Shokuhfar, A. Rezaei, S. Ahmadi, Defect and Diffusion Forum 258-260, (2006), 20-25.
20. V. G. Davydov, J. N. Fridlyander, M. V. Samarina, A. I. Orozov and L. B. Ber, Mater. Sci. Forum, 331-337, (2000), 1049-1054.